



Application of Digital Image Correlation for the effect of glass fibres on the strength and strain to failure of polyamide plastics

V. Crupi, E. Guglielmino, G. Risitano, F. Tavilla

Università degli Studi di Messina, Dipartimento di Ingegneria Elettronica, Chimica e Ingegneria Industriale, Contrada Di Dio (S. Agata), 98166 Messina (Italy)

crupi.vincenzo@unime.it, eguglie@unime.it, ftavilla@unime.it

ABSTRACT. For many years short fibre reinforced polymers have been commercially very attractive, mainly because of their superior mechanical properties over corresponding polymer matrices and their low-cost fabrication technique. Owing to their complex microstructure, especially in relation to fibre length and orientation distributions, an understanding of strength has not been well established. The aim of the present study is the investigation of the mechanical performance of injection moulded short glass fibre-reinforced polyamide composites. The glass fibre content of these composites was 35% by weight. Mono axial static tests were carried out. Specimens of the same material have been tested at different time starting from their production in order to analyse the natural ageing of the investigated composite material. The Digital Image Correlation (DIC) technique was applied during the tensile tests in order to obtain the stress-strain curves and to detect the failure zone at the early stages of the tests. From the experimental investigation, it results that there is a worsening of mechanical properties due natural aging of the test material.

SOMMARIO. Per molti anni, i materiali polimerici rinforzati con fibre corte sono stati molto interessanti dal punto di vista commerciale, soprattutto grazie alle loro proprietà meccaniche superiori alle corrispondenti matrici polimeriche ed alla loro tecnica di fabbricazione a basso costo. A causa della loro microstruttura complessa, soprattutto in relazione alla lunghezza e distribuzione delle fibre, non vi è ancora un'adeguata comprensione della loro resistenza meccanica. L'obiettivo del presente studio è l'analisi delle proprietà meccaniche di questi materiali. Il contenuto in fibra di vetro dei compositi investigati è pari al 35% in peso. Sono state effettuate prove statiche di trazione. Provini dello stesso materiale sono stati testati in tempi differenti a partire dalla data della loro produzione, al fine di analizzare il "naturale invecchiamento" del materiale composito indagato. La tecnica di correlazione delle immagini digitali (DIC) è stata applicata durante le prove di trazione al fine di ottenere le curve sforzo-deformazione e per rilevare la zona di rottura già nelle fasi iniziali dei test. Dall'indagine sperimentale, risulta che vi è un peggioramento significativo delle proprietà meccaniche dovute al naturale invecchiamento del materiale di prova.

KEYWORDS. Short Fibre Reinforced Polymers; Digital Image Correlation; Tensile Properties.

INTRODUCTION

Polyamide-6,6 is one such engineering thermoplastic which is known for its balance of strength, modulus and chemical resistance. Both polyamide-6,6 and short E-glass fibre reinforced polyamide-6,6 composite have many potential applications, such as stressed functional automotive parts (fuel injection rails, steering column switches), safety parts in sports and leisure (snowboard bindings) and other commercial products where creep resistance, stiffness,



resistance to dynamic fatigue and some toughness are demanded in addition to weight saving. The E-glass fibres give the composite its stiffness and strength and polyamide-6,6 matrix provides the means for achieving toughness and chemical resistance in addition to holding the fibres together.

Injection moulding of short-fiber-reinforced thermoplastics combines these inherent processing advantages of injection moulding with the superior performance characteristics of composite materials (high strength-to-weight ratio, high stiffness, and possibly controlled anisotropy). Flow of a fiber suspension during injection moulding results in a preferential orientation of short fibers. This flow-induced fiber orientation can vary significantly across the thickness of injection-molded parts. In the injection moulding of thin parts, the flow near the walls tends to be shear dominated, whereas near the mid-plane, the flow is extensional-flow dominated since the shear vanishes along the midplane in the symmetric case. This extensional flow can be especially significant near a point gate, such as for a center-gated disk. Owing to this shearing/stretching nature of the flow in injection moulding, the fibers tend to be aligned transverse to the flow near the mid-plane (core region) but aligned with the flow near the surface (shell region). As the composite solidifies, this flow-induced orientation of short fibers is frozen into the matrix and becomes a key feature of the finished product.

Even though the strength of short-fiber composites is lower and less anisotropic than that of long fiber composites, prediction of fiber orientation in short fiber-reinforced injection-molded (SFRIM) parts is still important for good structural design, to account for anisotropy in such properties as the elastic moduli and thermal-expansion coefficients of such products.

The tensile strength and toughness/impact energy of short fiber reinforced polymer composites would depend on a number of factors such as fiber length, interfacial adhesion and properties of components.

Risitano et al. [1] carried out numerical simulations and experimental tests for the modal analyses of a PA66GF35 plate. They have demonstrated that the vibration modes are closely related to the anisotropy of the material and the assumption of considering the material as isotropic leads to inevitable mistakes.

In [2] preliminary tests were performed to get information on the effects of manufacturing techniques of the specimens and test parameters, carried out in order to characterize fatigue resistance of PA66GF35. The trend of the surface temperature of the specimen was analyzed at different test frequencies. The load was maintained at a constant level below the fatigue limit in order to obtain an indication on the amount of energy converted into heat due to the only internal damping, which is strongly present for the viscoelastic nature (linear) of the material itself.

An energy-based approach was proposed by Meneghetti and Quaresimin [3] to analyse the fatigue strength of plain and notched specimens made of a short fiber-reinforced plastic weakened by rounded notches.

Thomason [4] has developed an improved method for obtaining the micromechanical parameters, interfacial shear strength, fibre orientation factor, and fibre stress at composite failure using input data from macromechanical tests. He measured the mechanical properties and residual fibre length distributions of glass fibre reinforced polyamide 6,6 containing different levels of glass fibre (0%, 4%, 10%, 20%, 30% and 40% by weight). These data were used as input for the model. The trends observed for the obtained resultant micromechanical parameters were in good agreement with the values obtained by other methods [5-8].

In [9] tensile properties and notched Charpy impact energy of injection-molded rubber-toughened polyamide 6,6/polypropylene (PA6,6/PP) blends reinforced with short glass fibers were studied. The glass fiber content was fixed at 40 wt%. The polymer blends containing various PA6,6/PP ratios, plus a mixture of 10 wt% styrene-ethylene-butylene-styrene and 10 wt% maleic anhydride grafted SEBS (SEBS-g-MA), were formulated. Two types of E-glass fibers were used to examine the influences of PA6,6/PP ratio on mean fiber length and critical fiber length and in turn on the mechanical properties. The PA6,6/PP ratio was found to have significant effects on both the mean fiber length and the critical fiber length in the final samples, and then on the mechanical properties. It was shown that the composite strength increased while the elastic modulus decreased with increasing PA6,6/PP ratio. This observation has been explained using the variance of interfacial adhesion and fiber length with the PA 6,6/PP ratio. The tensile failure strains were higher for the glass fiber-reinforced SEBS/SEBS-g-MA toughened blends than for glass fiber-reinforced toughened PA6, 6 or PP composites. The notched Charpy impact energy of the reinforced blends at a medium (75/25) PA6,6/PP ratio was exhibited to be higher than for the reinforced rubber-toughened PA6,6 or PP composites. Consequently, it was concluded that control of the PA6,6/PP ratio would be an effective way to produce composites with optimal combination of superior overall mechanical properties.

An investigation of the mechanical performance of injection moulded long glass fibre-reinforced polyamide 6,6 composites is presented in [10]. The glass fibre content in these composites was varied over the range 10–50% by weight using fibres with average diameters of 10, 14, and 17 μm . Mechanical testing and analysis of the apparent interfacial shear strength was carried out at 23 and 150 $^{\circ}\text{C}$ on dry-as-moulded and boiling water conditioned samples. The results from these composites are compared with standard extrusion compounded short glass fibre materials. The influence of fibre



diameter and concentration on the residual fibre length, fibre orientation distribution and composite strength and elongation to failure is presented and discussed in comparison to the predictions of some of the available micromechanical models.

In [11] the tensile properties of different grades of a short fibre reinforced polyamide, having various contents of glass fibres, were analysed. The fibre length distributions, obtained by optical microscope observations of the fibres extracted from the matrix, were statistically analysed and compared. The tensile behaviour of the different materials was modelled by applying micro-mechanical models, taking into account the fibre length distributions. The effect of the fibre content on the fibre orientation distribution is discussed on the basis of the analysis of the reconstructions of the internal fibre structure by micro tomography using synchrotron light. The relationship between the degree of anisotropy and the orientation factors used in the models is discussed.

Ghorbel et al. [12] analysed the temperature field evolution of glass fibers reinforced polyamide 6,6 with 0%, 10%, 20% and 30% glass fiber. In addition to infrared thermography, digital image correlation (DIC) was used to quantify deformation localization zones and correlate them to identified heat dissipation sources. The thermal response of short fiber reinforced materials was found to differ markedly from the uncharged one. Strong heterogeneity of the thermal was observed and was associated to localisation processes at different scales (investigated by DIC). The effect of the applied strain rate on the observed thermal heterogeneities was investigated. In addition to DIC, the volume damage evolution was monitored using X-ray computed microtomography in particular region.

The DIC technique, used in the past [13] by some of the authors for the analysis of steel welded joints, was applied in the present study to verify whether the DIC technique can give useful indications for SFRIM materials. Mono axial static tests were carried out on PA66 GF35 (polyamide-6,6 containing 35 wt% glass-fibres). Specimens of the same material have been tested at different time starting from their production in order to analyse the natural ageing of the investigated composite material. The stress-strain curves were obtained using the Digital Image Correlation (DIC). This technique was able to predict the failure zone already in the early stages of the tests at low values of load.

MATERIAL AND METHODS

A characteristic of SFRIM materials is their high degree of anisotropy, caused by fiber orientation. An injection molded SFRIM plate has a layered structure. Skin, shell, and core layers are distinguished, with orientations usually random, in the mold flow direction (MFD) and perpendicular to MFD respectively. The orientation in these layers and the thickness of the layers vary from location to location in the plate. Therefore, the properties of the material vary throughout the plate. For example, the tensile strength of specimens cut from a plate can vary between 100 and 160 MPa [14]. This depends on the locations where the specimens are cut, and the direction of the axis of the specimens relative to the MFD. The modulus of elasticity of the specimens varies in approximately the same degree as the strength.

Short fibers in a composite cannot be directly loaded at their ends and stress must be therefore transferred into them by shear forces at the fiber–matrix interface [15]. If the fibers are shorter than some critical length, l_c , so that the ineffective length (half of the length of a short fiber), δ , is less than $l_c/2$, the level of stress that can be transferred into the fibers will never reach the fiber failure stress and such short fibers can never be broken by loading the composite. The critical fiber length, $l_c = 2\delta$ thus represents the shortest fiber that can be broken. In other words, if $l_c > 2\delta$ the fiber will be pulled out at the fracture surface and the fiber pullout length must be shorter than $l_c/2$. If $l_c < 2\delta$, the fiber will likely be broken and the maximum fiber pull-out length should be equal to $l_c/2$; otherwise, the fiber will be further broken.

Various researchers have studied the failure mechanism either in tensile experiments or in fatigue [14]. Although for tensile experiments, conclusions are generally the same for various materials, for fatigue this is not the case.

In tensile experiments the failure mechanism is generally assumed to consist of the following steps [16]:

1. cracks initiate at fiber ends;
2. cracks propagate in the matrix along the interface, thus leaving a thin layer of matrix material adhered to the fiber. Only in systems with poor fiber-matrix bonding does the interface itself fail;
3. matrix cracks grow from the interfacial cracks, possibly after generation of matrix plastic deformation [17].

The tensile strength and failure strain of SFRIM would depend on a number of factors; the most usually important are:

- wt% of fiber (e.g. PA6 GF10, PA6 GF20, PA6 GF30) [11] (Fig. 1);
- crosshead rate (e.g. PA66 GF33) [18] (Fig. 2);
- test temperature (e.g. PA66 GF33) [19] (Fig. 3);



- test wetness (e.g. PA66 GF30, PA66 GF40) [10] (Fig. 4).
Furthermore, for the same material (e.g. PA6 GF30) and authors [11, 20] the mechanical characteristics (tensile strength, elastic modulus and failure strain) have a large dispersion of data (Fig. 5).

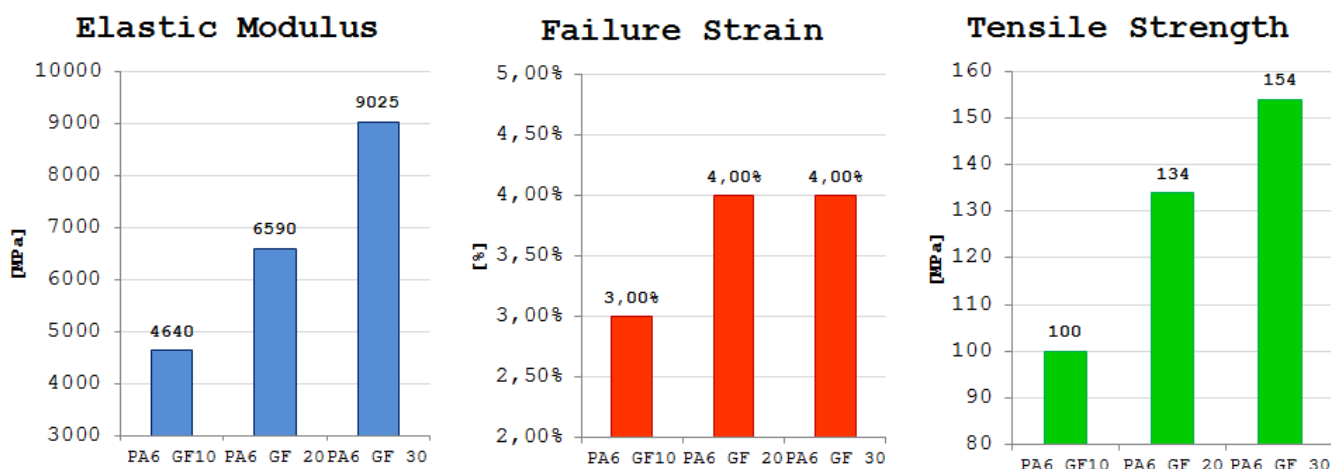


Figure 1: Different mechanical characteristics (elastic modulus, failure strain, tensile strength) depended on wt% of fiber (PA6 GF10, PA6 GF 20, PA6 GF30).

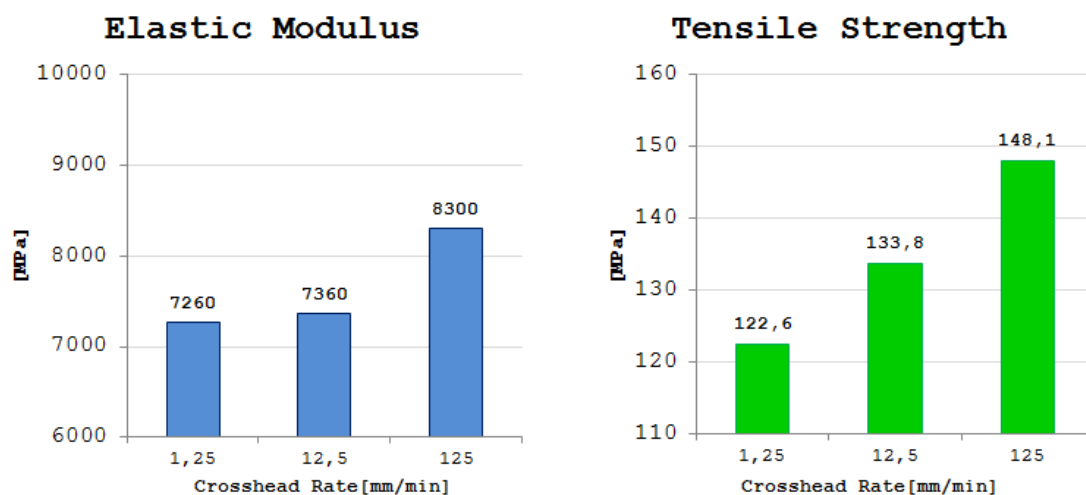


Figure 2: Different mechanical characteristics (elastic modulus, tensile strength) depended on crosshead rate of PA66 GF33.

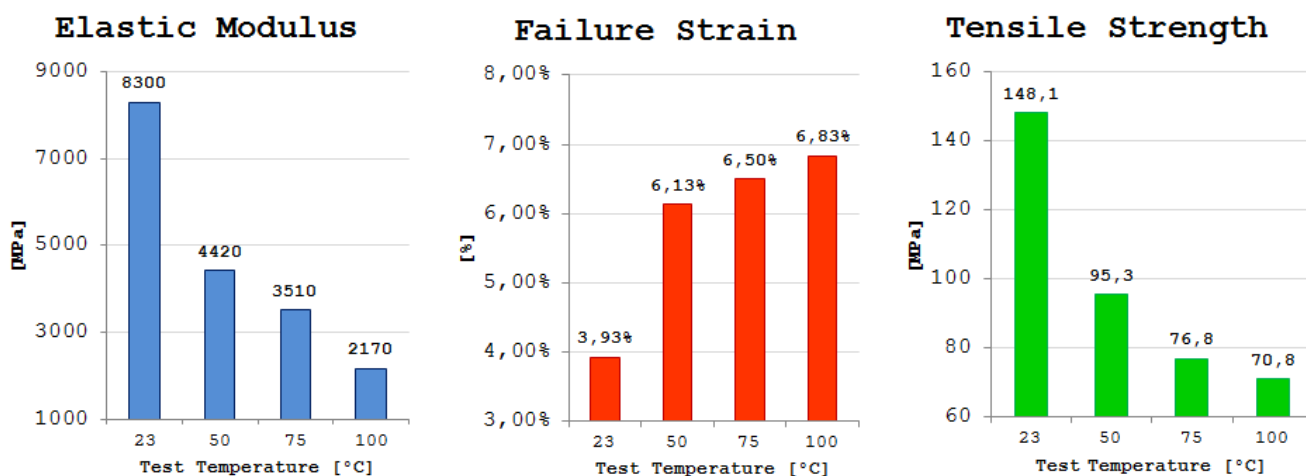


Figure 3: Mechanical characteristics (elastic modulus, failure strain, tensile strength) depended on test temperature of PA66 GF33.

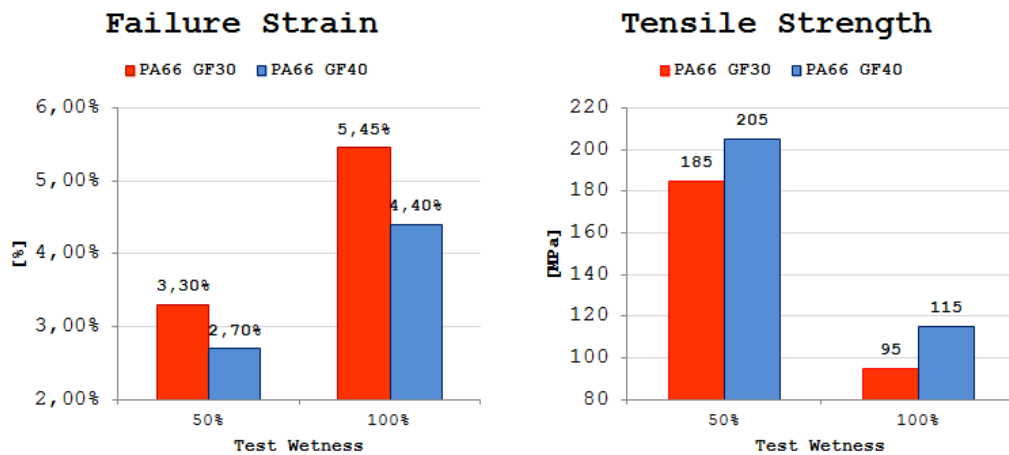


Figure 4: Mechanical characteristics (failure strain, tensile strength) depended on test wetness of PA66 GF30 and PA66 GF40.

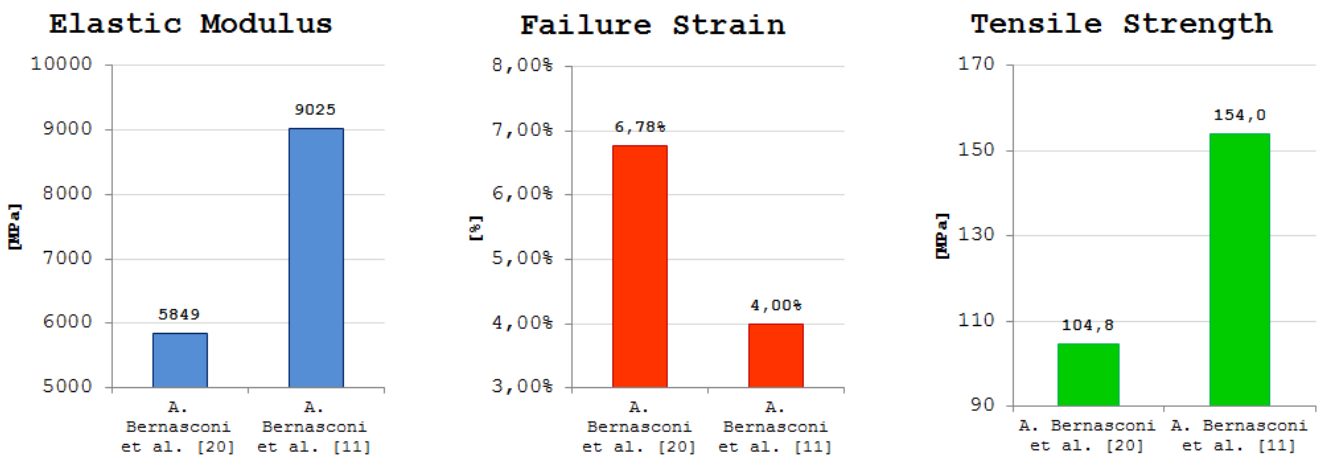


Figure 5: Mechanical characteristics (elastic modulus, failure strain, tensile strength) for PA6 GF30.

The material used in this study is a commercial polyamide-6,6 containing 35 wt% glass-fibres. It was used to produce moulded composites with 35% wt glass content (the glass fibre content was based on total mass of polymer). It was designed as PA66 GF35. Tab. 1 shows the mechanical and physical properties of the material (values extracted from the manufacturer's datasheet). The specimens were made by injection moulding. Granulated commercial materials were held in a drying furnace at $60\text{ }^{\circ}\text{C} \div 80\text{ }^{\circ}\text{C}$ for 24h prior to injection. For all blends, the injection parameters were maintained constant.

Material	Fiber Diameter [μm]	Fiber Length [μm]	Density [kg/m^3]	Specific Heat Capacity [$\text{kJ}/(\text{kg}\cdot\text{K})$]	Tensile Strength [MPa]	Elastic Modulus [MPa]	Failure strain [%]
PA66 GF35	10	280	1410	1.5	150 \div 210	8700 \div 11400	3 \div 4

Table 1: Mechanical and physical properties of the material PA66 GF35 according to the manufacturer's datasheet.

The tests were carried out using a servo-hydraulic load machine at a crosshead rate equal to 2 mm/min with constant relative humidity and temperature. Specimens were tested "dry as moulded". The tensile tests were carried out on 17 specimens (Fig. 6), relative to different time (1, 77, 100, 150 days) starting from their production in order to analyse the natural ageing of the investigated composite material. For each testing condition, several samples were used and at least three results were taken from those specimens in which the failure occurred within the gauge length. Tensile strength, modulus of elasticity, percent elongation to failure were determined by the tensile tests.

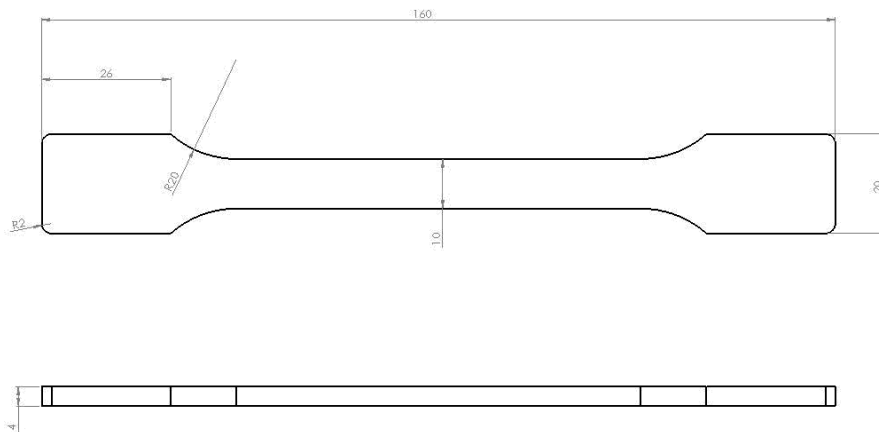


Figure 6: Geometry and dimensions of the specimen [mm].

Digital Image Correlation (DIC) is a data analysis method which uses a mathematical correlation to analyse digital images of samples subjected to mechanical strain [21, 22]. A detailed description of the DIC techniques is beyond the scopes of this paper, therefore, only a brief introduction is given in the following. The surface of the specimen is marked with a number of small speckles, in order to obtain a random pattern. As the specimen is loaded, consecutive images captured during the test register a change in surface characteristics. The basic idea is to analyse the surface aspect of the specimen before and after the loading, in order to estimate the field of motion of the random pattern and, consequently, of the surface of the specimen. Considering two subsequent images of the marked specimen, acquired at different loads, the first one is split into rectangular areas, region of interest, of fixed size. Once the regions of interest are defined, the DIC algorithm can be applied to each area of the first image, looking for the second image portion which is the “most similar” to the starting area, i.e. for the region that corresponds to the minimum value of a proper figure of merit. With the DIC technique it is possible to estimate the displacement field in each region of the specimen; from this information the strain field can be derived.

In this paper, ARAMIS 3D 2M LT system was used to analyze the strain pattern of the specimen surface. Two cameras with a resolution of 1600 x 1200 pixel were used. The system accuracy for the strain measurement is about 10^{-4} , while the higher acquisition frequency is 12 Hz.

RESULTS & DISCUSSION

Tensile properties were measured in accordance with the procedures in UNI EN ISO 527 at a crosshead rate of 2 mm/min. Specimens of the same material (PA66 GF35) have been tested at different time starting from their production. During the static experiments carried out after several days (77, 100, 150 days), the displacements of the specimens were monitored by DIC technique, enabling the calculation of elastic modulus and strain.

Tensile strength vs time curve are shown in Fig. 7. There is a high reduction of tensile strength in the course of time; in 150 days, the value of the tensile strength decreases by about 30%. This result reflected an industrial feedback; it is not uncommon in the industrial field the case where some SFRIM components lose their stiffness and strength characteristics in a short time life. This type of drawback involves an inevitable additional cost to the redesign of a new component that takes into account the characteristics of the material changing in time. In Fig. 7, in addition to the experimental values of the tensile strength, the values reported in the literature [4, 10] (the tests were carried out at a crosshead of 2 mm/min) and in the manufacturer’s datasheet are shown. It may be noted that the tensile strength of the “new” material (1 day) is in accordance with the data presented in literature [4, 10] and datasheet. Over time, the tensile strength decreases and becomes close to the minimum value of the manufacturer’s datasheet (100 days), deviating highly from the values of literature. The material is “transformed into another material” after 150 days, having an average value (AVG) of the tensile strength totally different from the one of the original material (AVG $\sigma_{1 \text{ day}} = 190 \text{ MPa}$ vs AVG $\sigma_{150 \text{ day}} = 133 \text{ MPa}$).

Fig. 8 shows tensile strength vs strain failure curves of three different tests for 77, 100 and 150 days, which confirm that over time the material loses its mechanical characteristics. The curves at 77 days (red diamonds) and 150 days (blue squares) are so different that seem to belong to two distinct materials.

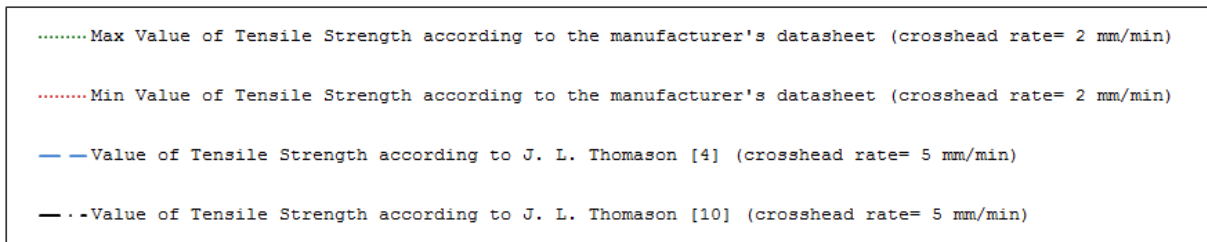
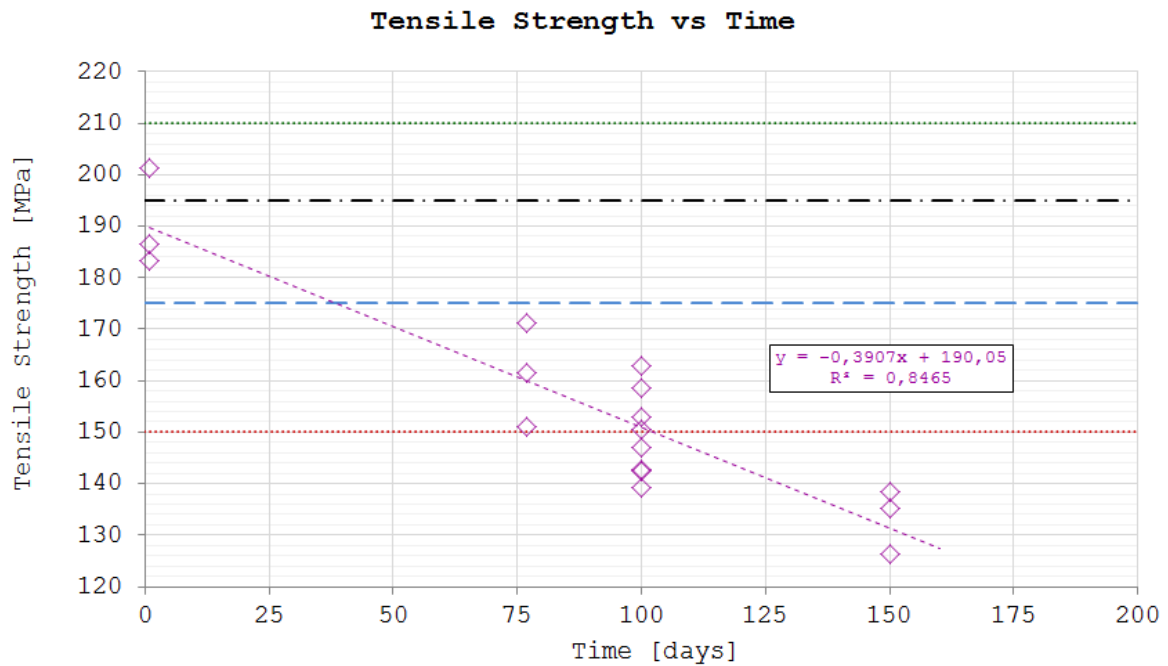


Figure 7: Tensile strength vs time.

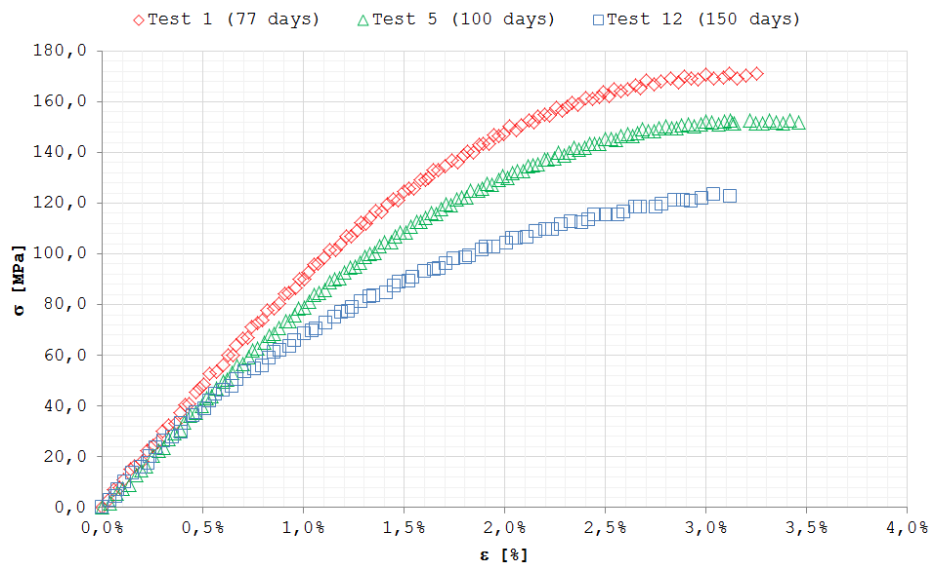


Figure 8: Tensile strength vs strain failure for three different test ($v = 2 \text{ mm/min}$).

Fig. 9 shows the trend of the elastic modulus vs time. It may be noted that up to 100 days the elastic modulus is similar to the values presented in the literature [4] (the tests were carried out at a crosshead of 2 mm/min) and in the datasheet. Instead, to 150 days the value of the elastic modulus decreases highly, losing 15% of stiffness compared to the minimum value presented in the manufacturer's datasheet. Fig. 10 shows the trend of strain failure vs time. Unlike the values of

tensile strength and elastic modulus, the values of the strain failure are in agreement with the data presented in the manufacturer's datasheet and are in media with the values presented in the literature (slightly higher than [4]). This result shows that the strain of this material is not a function of time, unlike the other mechanical characteristics. Fig. 9 and 10 report the data obtained by the tests, which produced the average values and in which DIC technique was applied.

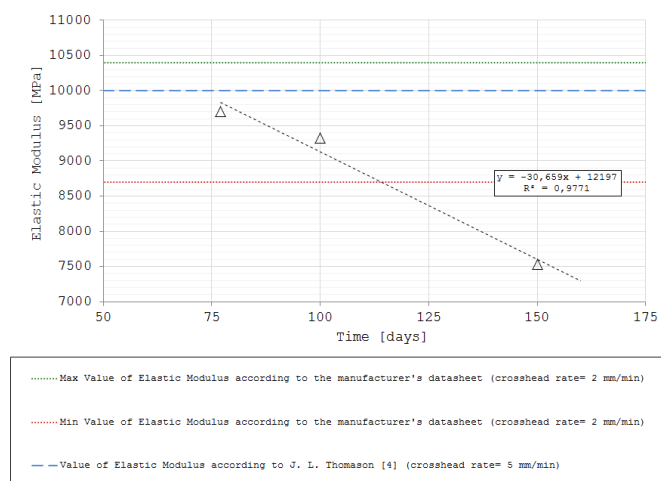


Figure 9: Elastic modulus vs. time.

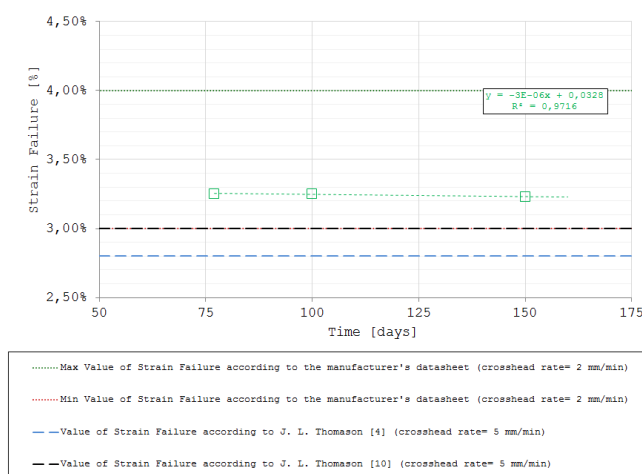


Figure 10: Strain failure vs. time.

As mentioned earlier, ARAMIS 3D 2M LT system was used to analyze the strain pattern of the specimen surface. Since with the DIC technique it is possible to estimate the displacement field in each region of the specimen, this technique was applied during the tensile tests in order to obtain the stress-strain curves and in addition to detect the failure zone at the early stages of the tests. In Fig. 11, an application of DIC technique during a tensile test is showed. In the figure, with the stress vs strain curve, some images obtained by DIC analysis at different stage points are showed; magnification of the images was done in order to understand the evolution of strain in the future fracture zone. In Fig. 12, for the same test, a greater number (10 stage points) of magnified images has been reported.

Analysing the Fig. 11 and 12, it can be noted that even at low strain (0,4%) it's possible pinpoint the future fracture zone. For all stage point, the evolution of strain is constant and give a good indication where there should be the failure zone. As mentioned earlier, a characteristic of SFRIM materials is their high degree of anisotropy, short fibers cannot be directly loaded at their ends and stress must be therefore transferred into them by shear forces at the fiber–matrix interface. Furthermore, in tensile experiments it is generally assumed that cracks initiate at fiber ends and propagate in the matrix; such matrix cracks grow following the generation of matrix plastic strain, within the interfacial cracks. From the analysis made, it appears that the DIC technique can be used with success to identify areas in which the fiber-matrix interface is more sensitive. Indeed, the images at several stage points identified as area most stressed always the same; this area is the one where the specimen breaks at the end of the test.

CONCLUSIONS

The SFRIM composites are very attractive materials in the industrial field for their interesting properties, but a knowledge of their mechanical properties is necessary for a correct use of these materials. The analysis of their tensile strength was investigated using the full field technique, based on digital image correlation. Specimens of the same material have been tested at different time starting from their production.

The experimental tests showed that:

- the investigated materials are subjected to a natural aging with an high reduction of their strength;
- the investigated materials are subjected to a natural aging with a reduction of their elastic modulus;
- the strain of the investigated material is not a function of time, unlike the other mechanical characteristics;
- the DIC technique was able to predict the fracture zone already at the first stage of the tests even at low values of strain.

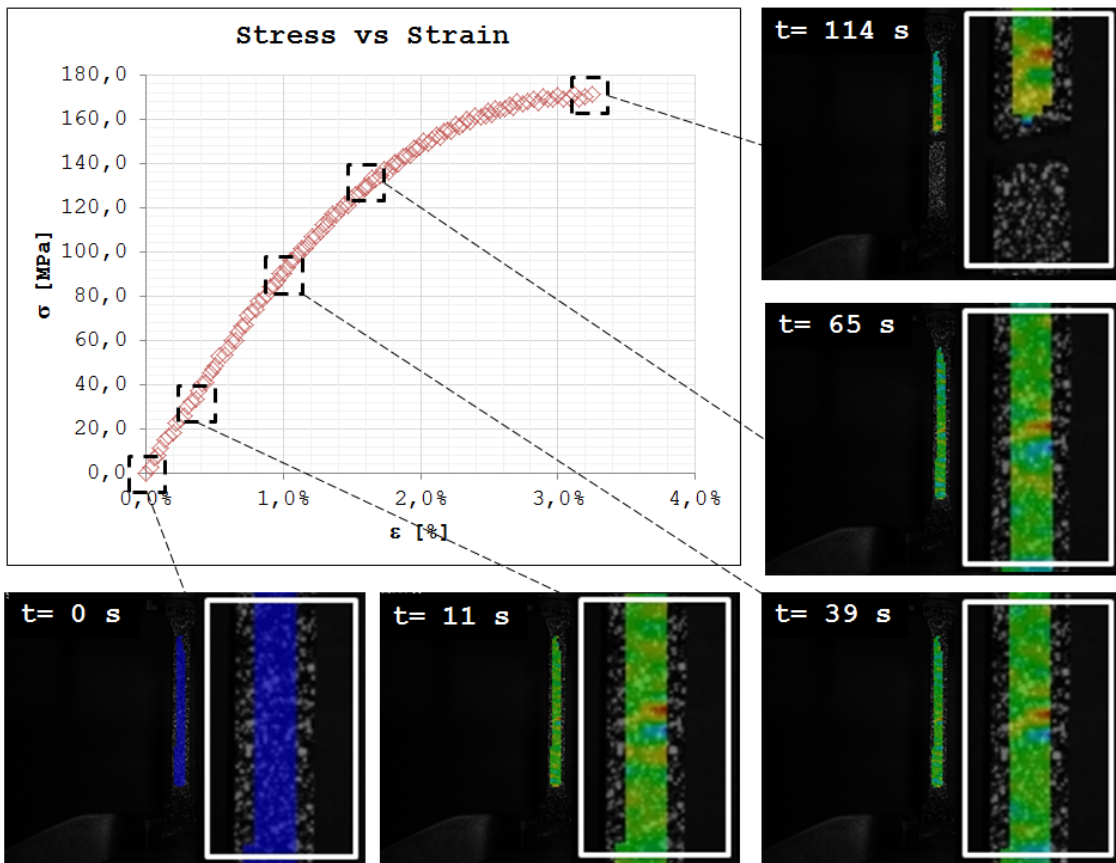


Figure 11: Example given of DIC analysis for tensile test.

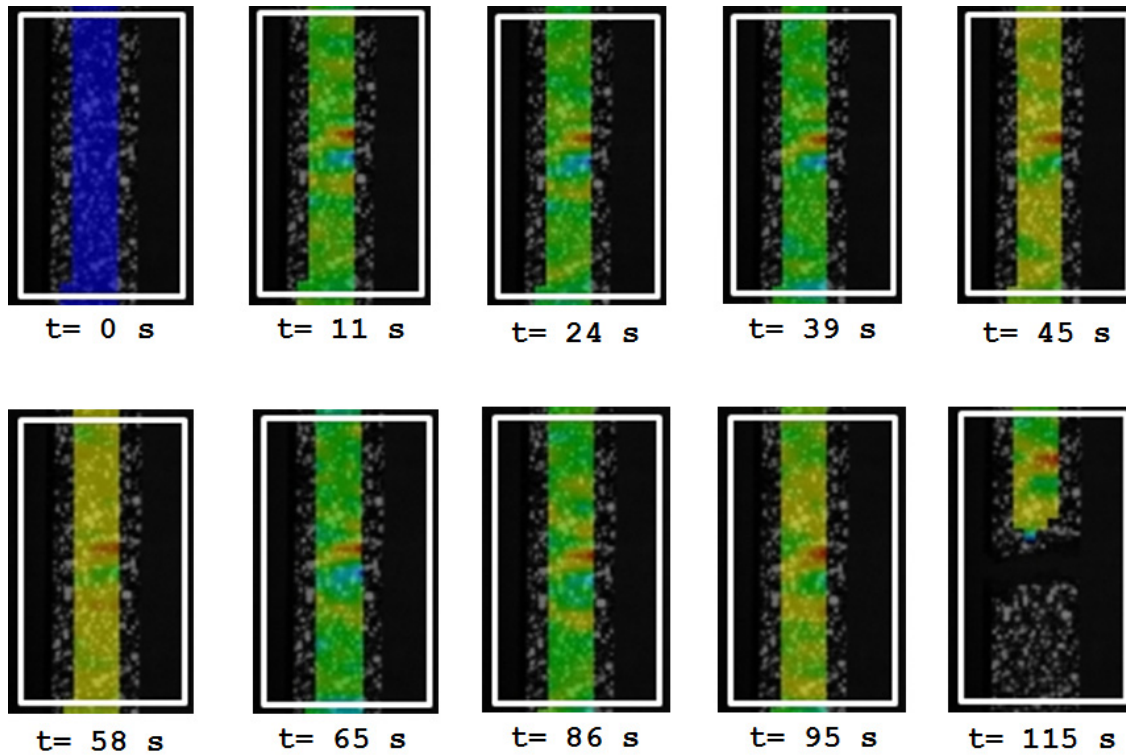


Figure 12: Detail DIC images at progressive time test for tensile test (Fig. 11).



REFERENCES

- [1] G. Risitano, D. Corallo, F. Sellani Langarelli, A. Davitti, N. Bellato, In: Workshop IGF, Forni di Sopra, Italy, (2012).
- [2] G. Risitano, D. Corallo, L. Scappaticci, D. Dozzo, N. Bellato, In: 41° Congresso Nazionale AIAS, Vicenza, Italy, (2012).
- [3] G. Meneghetti, M. Quaresimin, *Composites: Part B*, 42 (2011) 217.
- [4] J.L. Thomason, *Compos. Sci. Technol.*, 61 (2001) 2007.
- [5] W. H. Bowyer, M. G. Bader, *J. Mater. Sci.*, 7 (1972) 1315.
- [6] W. H. Bowyer, M. G. Bader, *Composites*, 4 (1972) 150.
- [7] S. Toll, P. O. Andersson, *Composites*, 22 (1991) 298.
- [8] R. S. Bay, C. L. Tucker, *Polym. Eng. Sci.*, 32 (1992) 240.
- [9] S. Y. Fua, B. Lauke, R. K. Y. Lid, Y. W. Mai, *Compos. Part B*, 37 (2006) 182.
- [10] J.L. Thomason, *Compos. Part A*, 39 (2008) 1618.
- [11] A. Bernasconi, F. Cosmi, *Procedia Engineering*, 10 (2011) 2129.
- [12] A. Ghorbel, N. Saintier, A. Dhiab, *Procedia Engineering*, 10 (2011) 2123.
- [13] V. Crupi, E. Guglielmino, L. Musumeci, In: 40° Congresso Nazionale AIAS, Palermo, Italy, (2011).
- [14] J. J. Horst, J. L. Spoomaker, *Polym. Eng. Sci.*, 36 (1996) 2718.
- [15] D. Harris, *Engineering Composite Materials*, London: The Institute of Metals, U.K. (1986).
- [16] N. Sato, S. Sato, T. Kurauchi, In: Fourth Intl. Conf. on Composite Materials, ICCM-W, Tokyo, Japan, (1982).
- [17] N. Sato, T. Kurauchi, O. Kamigaito, In: 7th Int. Con. on Deformation, Yield and Fracture of Polymers, Cambridge, U.K., (1988).
- [18] P.K. Mallick, Y. Zhou, *Int. J. Fatigue*, 26 (2003) 941.
- [19] Y. Zhou, P.K. Mallick, *Polym. Compos.*, 27 (2006) 230.
- [20] A. Bernasconi, M. Broznic F. Cosmi, D. Dreossi, G. Tromba, In: IGF19, Milano, Italy, (2007).
- [21] T. C. Chu, W. F. Ranson, M. A. Sutton, W. H. Peters, *Exp. Mech.*, 25 (1985) 232.
- [22] H. Po-Chih, A. S. Voloshin, *J. of the Braz. Soc. of Mech. Sci. Eng.*, 25 (2003) 215.